

# A Genome-Wide Transcriptional Analysis of the Mitotic Cell Cycle

Raymond J. Cho,\*# Michael J. Campbell,†#||  
Elizabeth A. Winzeler,† Lars Steinmetz,\*  
Andrew Conway,† Lisa Wodicka,†  
Tyra G. Wolfsberg,§ Andrei E. Gabrielian,§  
David Landsman,§ David J. Lockhart,†  
and Ronald W. Davis\*†

\*Department of Genetics

†Department of Biochemistry  
Stanford University School of Medicine  
Stanford, California 94305

‡Affymetrix

3380 Central Expressway  
Santa Clara, California 95051

§National Center for Biotechnology Information  
National Library of Medicine  
Bethesda, Maryland 20894

## Summary

Progression through the eukaryotic cell cycle is known to be both regulated and accompanied by periodic fluctuation in the expression levels of numerous genes. We report here the genome-wide characterization of mRNA transcript levels during the cell cycle of the budding yeast *S. cerevisiae*. Cell cycle-dependent periodicity was found for 416 of the 6220 monitored transcripts. More than 25% of the 416 genes were found directly adjacent to other genes in the genome that displayed induction in the same cell cycle phase, suggesting a mechanism for local chromosomal organization in global mRNA regulation. More than 60% of the characterized genes that displayed mRNA fluctuation have already been implicated in cell cycle period-specific biological roles. Because more than 20% of human proteins display significant homology to yeast proteins, these results also link a range of human genes to cell cycle period-specific biological functions.

## Introduction

The events of DNA replication, chromosome segregation, and mitosis define a fundamental periodicity in the eukaryotic cell cycle. Precise coordination of the unidirectional transitions between these stages is critical to cell integrity and survival. Loss of appropriate cell cycle regulation leads to genomic instability (Hartwell and Kastan, 1994) and is believed to play a role in the etiology of both hereditary and spontaneous cancers (Hunter and Pines, 1994; Wang et al., 1994; Sherr and Roberts, 1995; Wölfel et al., 1995; Hall and Peters, 1996). Cell cycle-dependent mRNA fluctuation has been observed for genes involved in many cellular processes,

including control of mRNA transcription (Wittenberg et al., 1990; Oehlen et al., 1996), responsiveness to external stimuli (Zanolari and Riezman, 1991; Oehlen and Cross, 1994), and subcellular localization of proteins (Scully et al., 1997). Genetic studies have revealed that the activity of cell cycle-regulatory proteins is required for normal DNA repair (Painter and Young, 1980; Weinert and Hartwell, 1988; Weinert, 1997), meiosis (Jang et al., 1995; Verlhac et al., 1996), and multicellular development (Gönczy et al., 1994; Thomas et al., 1994, 1997; Dong et al., 1997). These observations suggest that all eukaryotic cells experience important physiological changes during the cell cycle, and that diverse biological events depend on maintenance of this periodicity.

The numerous biological changes associated with the cell cycle make it an attractive model for the study of genome-wide regulation of gene activity. Parallel identification of all of the genes in a genome that are coordinately regulated during such a process provides a consistent internal standard for comparison of gene activity over time and makes it possible to search statistically for candidate regulatory sequences. Although the cell cycle-dependent regulation of many individual genes has been studied, comprehensive results for a genome are likely to reveal novel functional and physical organization in coordinate gene regulation. These results also provide an opportunity to identify related genes in the human genome that may be involved in cell cycle period-specific roles.

One of the key mechanisms of gene regulation takes place on the level of mRNA transcription. Availability of complete sequence for the *Saccharomyces cerevisiae* genome has made it possible to quantitate mRNA transcript levels for virtually every yeast gene (DeRisi et al., 1997; Wodicka et al., 1997). In this study, commercially available high-density oligonucleotide arrays were used to quantitate mRNA transcript levels in synchronized yeast cells at regular intervals during the cell cycle. DNA oligonucleotide probes are directly synthesized on these arrays without individual manipulation or PCR amplification, minimizing the potential for cross-hybridization or clone error (Lashkari et al., 1997).

## Results and Discussion

To obtain synchronous yeast culture, *cdc28-13* cells were arrested in late G1 at START by raising the temperature to 37°C, and the cell cycle was reinitiated by shifting cells to 25°C. Cells were collected at 17 time points taken at 10 min intervals, covering nearly two full cell cycles. Cells exhibited over 95% synchrony throughout the time course, as determined by bud size and nuclear position (Figure 1). Poly(A)<sup>+</sup> RNA was isolated from each sample, converted to cDNA, labeled, and hybridized to yeast whole genome oligonucleotide expression arrays (Figure 2). To obtain cells synchronized in a different way, an isogenic strain bearing the *cdc15-2* allele, which enables arrest in late G2, was used to generate a second time course. Transcript levels from the *cdc15-2* arrest

|| To whom correspondence should be addressed (Present address: Molecular Applications, 607 Hansen Way, Building 1, Palo Alto, California 94304. E-mail: campbell@mag.com).

# These authors contributed equally to this work.

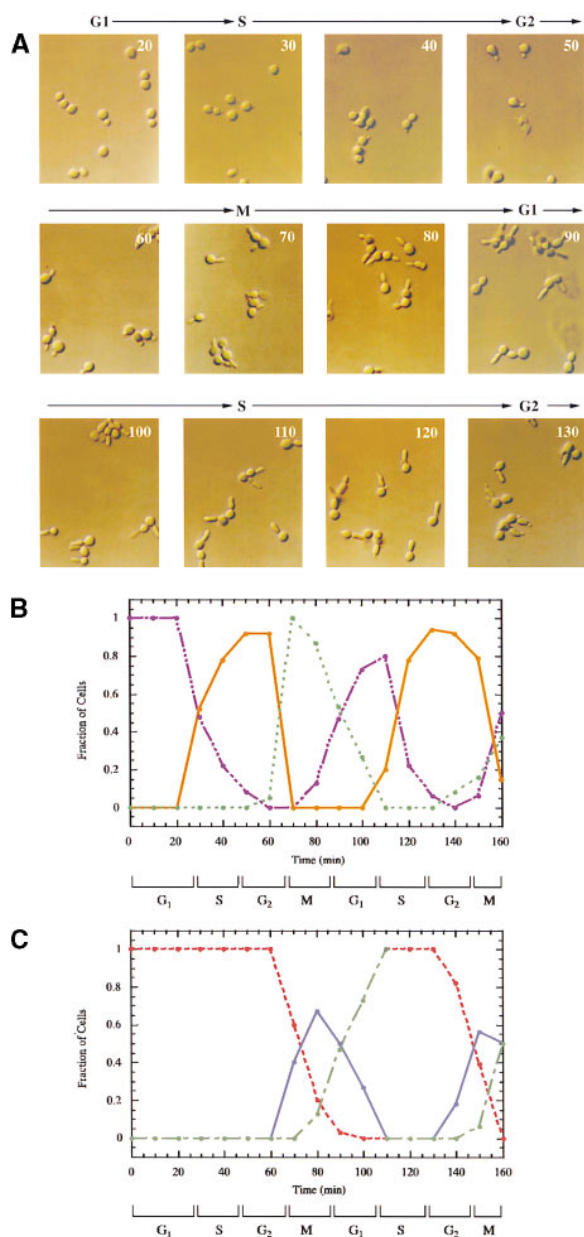


Figure 1. Synchrony of *cdc28-13* Cells

(a) Phase contrast photographs of *S. cerevisiae* cells (K3445 strain containing the *cdc28-13* allele) at various times following release from arrest.

(b) Graph of the percentage of cells that are unbudded (purple line), small budded (yellow line), and large budded (green line) versus time.

(c) Graph of the percentage of cells that are premitotic (red line), mitotic (blue line), and postmitotic (green line) versus time (obtained from DAPI). At the 110 min time point, virtually all cells were observed to have completed mitosis. (The junction between red and blue lines at this time point indicates the switch of cells from a postmitotic to a premitotic state.)

time course were also measured by hybridization to oligonucleotide arrays. More than 200 transcripts were visually compared between the two time courses. Transcript fluctuations from the two time courses generally showed good agreement. Overall, more than 85% of

fluctuations observed in the *cdc28-13* time course were discernable in the *cdc15-2* time course. Because a greater degree of cell synchrony was observed with the *cdc28-13* allele than with the *cdc15-2* allele, subtle fluctuations were more easily discerned in the *cdc28-13* time course. Graphs comparing mRNA fluctuation from both time courses are available at the WWW site <http://genomics.stanford.edu>.

Some differences in transcript levels could result from the shift between the restrictive and permissive temperatures and from the state of cell cycle arrest. To avoid temperature-induced effects unrelated to cell cycle progression, determination of cell cycle phase was based on data from *cdc28-13* time points taken more than 40 min past the point of release from arrest. The 1348 genes whose normalized mRNA level changed by more than 2-fold during this portion of the time course were visually examined for periodicity of expression in both the *cdc28-13* and *cdc15-2* strains. 416 genes were identified that demonstrated consistent periodic changes in transcript level (Table 1, Figure 3). This number represents approximately 7% of all yeast genes and agrees with previous estimates of the number of genes in *S. cerevisiae* that display cell cycle-dependent transcription (Koch and Nasmyth, 1994). The largest observed change in induction, 25-fold, was observed for both *CLN1* and *RNR1*. These changes are consistent with published results. The location of periodically transcribed genes was not observably biased toward any particular chromosome, and every chromosome contained at least one cell cycle-regulated gene. A data base containing a list of these genes, their relative mRNA fluctuations, and their functional classifications can be found at the WWW site described above.

The time course was divided into early G1, late G1, S, G2, and M phases based on the size of the buds, the cellular position of the nucleus, and standardization to more than 20 transcripts whose mRNA fluctuations have been previously reported (Figure 4) (Koch and Nasmyth, 1994). 134 of the 416 cell cycle-regulated transcripts peaked in late G1, while only 56 transcripts peaked during M phase. Transcripts that peaked in late G1 displayed particularly sharp rates of accumulation and decay, while transcripts that peaked in S generally displayed a less dramatic induction pattern. More than half of the transcripts that peaked in late G1, including the *CLN1* and *CLN2* cyclins, displayed a minor peak in G2. 13 out of 74 transcripts that peaked in S also displayed minor M peaks. The presence of minor peaks may indicate that a transcript is affected by more than one cell cycle-dependent regulatory sequence. An additional 33 of the 416 identified genes were induced in two different cell cycle phases, but did not display a predominant peak. This includes the cyclin-dependent kinase gene *CDC28*, which peaks twice, in G1 and G2. Genes displaying two transcriptional peaks were classified separately.

Identification and characterization of upstream regulatory sequences are critical to elucidating global mechanisms of transcriptional regulation. Several upstream regulatory sequences involved in cell cycle-dependent transcription have already been identified, including the late G1 elements MCB (MluI cell cycle box) and ECB

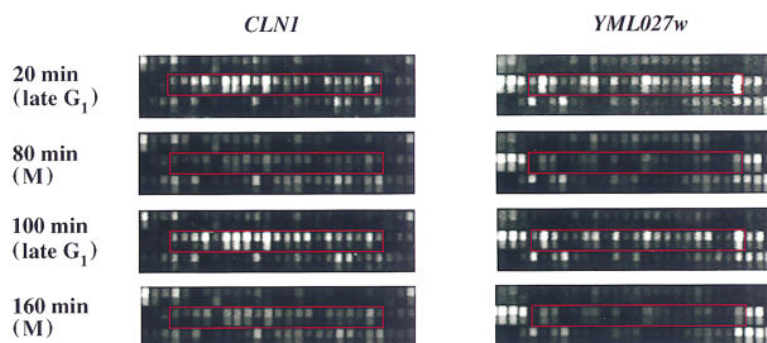


Figure 2. Transcript Hybridization to Whole Genome Oligonucleotide Arrays

Close-up views of high-density oligonucleotide arrays containing 25-mer probes for nearly every gene in the *S. cerevisiae* genome, following hybridization with labeled cDNA from samples 20, 80, 100, and 160 min past release from cell cycle arrest. The first column shows array features containing probes to the *CLN1* cyclin transcript, highlighted in red. The second column shows array features containing probes to the *YML027w* open reading frame. Transcript levels for both genes reached their maxima during late G1 phase.

(Swi4/6 cell cycle box) and the early G1 element SCB (early cell cycle box) (Nasmyth, 1985; Breeden and Nasmyth, 1987; Andrews and Herskowitz, 1989; McInerney et al., 1997). Of all genes with an MCB element within 500 bp of the start codon, 39% displayed periodic transcription in late G1 phase (Table 2). Of all genes with an ECB element within 500 bp of the start codon, 67% displayed periodic transcription in early G1 phase. However, only 7.4% of genes with an SCB element within 500 bp showed cell cycle-dependent transcription in late G1. The proportion of transcripts in the genome that is cell cycle regulated is 6.8%. Furthermore, a similar frequency of SCB elements was observed upstream of genes induced in cell cycle phases other than late G1. Therefore, the presence of an upstream SCB sequence is not predictive of periodic transcriptional fluctuation in late G1. One explanation for this observation is that the sequences adjacent to regulatory elements can negatively modulate their effects on transcription. Alternatively, these instances may represent transcripts that degrade too slowly to display sharp fluctuations in level during the cell cycle. Upstream regions of all genes were also searched for other known yeast regulatory sequences, including the *ABF1* and *RAP1* transcription factor binding sites. None of these sites were found with disproportionate frequency in the upstream regions of one class of cell cycle-regulated genes.

Other cell cycle period-specific transcription factors such as Swi5 do not have a highly conserved binding sequence, making it difficult to accurately search genomic sequence for possible sites of action (Breeden and Nasmyth, 1987; Ogas et al., 1991; Brazas and Stillman, 1993; McBride et al., 1997). However, it is unlikely that these binding sequences alone could completely account for the number of late G1 genes in which a known regulatory element could not be found. In addition, known cell cycle-regulatory sequences were observed rarely in the promoter regions of genes induced in G2, M, or S phase. Therefore, although these results indicate that the known cell cycle-regulatory sequences MCB and ECB have significant predictive value with regard to cell cycle-regulated transcription in the yeast genome, it is likely that the majority of upstream elements conferring cell cycle-specific transcription have yet to be identified.

The generation of a comprehensive list of coregulated genes makes it possible to statistically analyze a large set of promoter regions for previously undetected regulatory elements. A data base of potential transcriptional

regulatory sequences was created by extracting the 500 bp upstream of the translational start site of every gene in the genome. This data set was then searched for hexanucleotide and heptanucleotide sequences that occurred with disproportionate frequency in the upstream regions of one set of cell cycle-regulated genes. The two short sequences that displayed the greatest bias toward the promoter regions of genes in each cell cycle category are listed in Table 2 as candidate core sequences for new regulatory elements.

Some of these short sequences were then visually inspected to determine a longer consensus sequence. For example, the sequence 5'-GTAAACA-3' was found upstream of nearly 40% of the genes induced in G2 and M, but upstream of less than 14% of genes induced at other times. After visual inspection of several G2 and M gene upstream regions, this sequence was expanded to 5'-AAAANGTAAACAA-3'. A search of noncoding sequence revealed that this sequence was found upstream of 8% of genes induced in G2, but upstream of less than 0.2% of other genes in the genome (Table 2). Of all genes downstream of this sequence, 58% displayed transcriptional oscillation during the cell cycle.

Another method for identifying candidate regulatory elements is the examination of DNA sequences that have been previously implicated in cell cycle-dependent transcription, but for which a clear consensus sequence has not been established. For example, it has been shown that the MCM1 transcription factor plays a direct role in the induction of certain genes during G2 and M (Althoefer et al., 1995). The core MCM1 binding site 5'-CCYWWWNNGG-3' was examined in upstream regions of genes induced in G2 phase. The expanded core MCM1 binding sequence 5'-TWTNWCCYAAANNGGNN AAA-3' was observed within 1500 bp upstream of six genes induced during G2, but was not found again in the genome. Furthermore, nearly 20% of genes induced during G2 are downstream from similar putative MCM1 binding sites that are flanked by a T-rich region at the 5' end and an A triplet at the 3' end. Interestingly, the expanded site described above also resembles the constitutively bound MCM1 sites found upstream of the G2 genes *CLB1*, *CLB2*, *SWI5*, *BUD3*, and *BUD4* (Althoefer et al., 1995; Sanders and Herskowitz, 1996). Because no single sequence was found near a majority of genes induced in G2 and M, it is possible that a number of separate elements may be responsible for periodicity of mRNA abundance during these phases. Like the ECB

Table 1. Transcriptional Periodicity in Biologically Characterized Genes

<b>Early G1 phase (33/63)</b>	<b>Late G1 phase (81/134)</b>	<b>Repair and Recombination</b> YDL101c DUN1 YDR097c MSH6 YHR038w KIM4 YKL113c RAD27 YLR032w RAD5 YLR234w TOP3 YLR383w RHC18 YML021C UNG1 YML060w OGG1 YML061c PIF1 YNL082w PMS1 YOL090w MSH2 YPL153c SPK1	<b>Chromosome Segregation</b> YBL063w KIP1 YDR113c PDS1 YDR150w NUF1* YDR356w NUF1 YDR488c PAC11 YEL061c CIN8 YGR140w CBF2 YHR172w SPO97 YLR045c STU2 YMR198w CIK1 YNL126w SPC98 YOR026w BUB3 YPR141c KAR3	<b>Cell Cycle Regulation</b> YAL040c CLN3 YBR160w CDC28* YGL116w CDC20 YGR108w CLB1 YPR119w CLB2	<b>Chromosome Segregation</b> YBR138c HDR1 YDR150w NUF1* YGR092w DBF2 YHR023w MYO1 YOL069w NUF2 YOR058c ASE1 YPL242C IQG1	<b>Chromosome Segregation</b> YBR138c HDR1 YDR150w NUF1* YGR092w DBF2 YHR023w MYO1 YOL069w NUF2 YOR058c ASE1 YPL242C IQG1	<b>Chromosome Segregation</b> YBR138c HDR1 YDR150w NUF1* YGR092w DBF2 YHR023w MYO1 YOL069w NUF2 YOR058c ASE1 YPL242C IQG1	<b>Chromosome Segregation</b> YBR138c HDR1 YDR150w NUF1* YGR092w DBF2 YHR023w MYO1 YOL069w NUF2 YOR058c ASE1 YPL242C IQG1	<b>Chromosome Segregation</b> YBR138c HDR1 YDR150w NUF1* YGR092w DBF2 YHR023w MYO1 YOL069w NUF2 YOR058c ASE1 YPL242C IQG1	<b>Chromosome Segregation</b> YBR138c HDR1 YDR150w NUF1* YGR092w DBF2 YHR023w MYO1 YOL069w NUF2 YOR058c ASE1 YPL242C IQG1	<b>Chromosome Segregation</b> YBR138c HDR1 YDR150w NUF1* YGR092w DBF2 YHR023w MYO1 YOL069w NUF2 YOR058c ASE1 YPL242C IQG1	<b>Chromosome Segregation</b> YBR138c HDR1 YDR150w NUF1* YGR092w DBF2 YHR023w MYO1 YOL069w NUF2 YOR058c ASE1 YPL242C IQG1	<b>Chromosome Segregation</b> YBR138c HDR1 YDR150w NUF1* YGR092w DBF2 YHR023w MYO1 YOL069w NUF2 YOR058c ASE1 YPL242C IQG1	<b>Chromosome Segregation</b> YBR138c HDR1 YDR150w NUF1* YGR092w DBF2 YHR023w MYO1 YOL069w NUF2 YOR058c ASE1 YPL242C IQG1	<b>Chromosome Segregation</b> YBR138c HDR1 YDR150w NUF1* YGR092w DBF2 YHR023w MYO1 YOL069w NUF2 YOR058c ASE1 YPL242C IQG1	<b>Chromosome Segregation</b> YBR138c HDR1 YDR150w NUF1* YGR092w DBF2 YHR023w MYO1 YOL069w NUF2 YOR058c ASE1 YPL242C IQG1	<b>Chromosome Segregation</b> YBR138c HDR1 YDR150w NUF1* YGR092w DBF2 YHR023w MYO1 YOL069w NUF2 YOR058c ASE1 YPL242C IQG1	<b>Chromosome Segregation</b> YBR138c HDR1 YDR150w NUF1* YGR092w DBF2 YHR023w MYO1 YOL069w NUF2 YOR058c ASE1 YPL242C IQG1	<b>Chromosome Segregation</b> YBR138c HDR1 YDR150w NUF1* YGR092w DBF2 YHR023w MYO1 YOL069w NUF2 YOR058c ASE1 YPL242C IQG1	<b>Chromosome Segregation</b> YBR138c HDR1 YDR150w NUF1* YGR092w DBF2 YHR023w MYO1 YOL069w NUF2 YOR058c ASE1 YPL242C IQG1	<b>Chromosome Segregation</b> YBR138c HDR1 YDR150w NUF1* YGR092w DBF2 YHR023w MYO1 YOL069w NUF2 YOR058c ASE1 YPL242C IQG1	<b>Chromosome Segregation</b> YBR138c HDR1 YDR150w NUF1* YGR092w DBF2 YHR023w MYO1 YOL069w NUF2 YOR058c ASE1 YPL242C IQG1	<b>Chromosome Segregation</b> YBR138c HDR1 YDR150w NUF1* YGR092w DBF2 YHR023w MYO1 YOL069w NUF2 YOR058c ASE1 YPL242C IQG1	<b>Chromosome Segregation</b> YBR138c HDR1 YDR150w NUF1* YGR092w DBF2 YHR023w MYO1 YOL069w NUF2 YOR058c ASE1 YPL242C IQG1	<b>Chromosome Segregation</b> YBR138c HDR1 YDR150w NUF1* YGR092w DBF2 YHR023w MYO1 YOL069w NUF2 YOR058c ASE1 YPL242C IQG1	<b>Chromosome Segregation</b> YBR138c HDR1 YDR150w NUF1* YGR092w DBF2 YHR023w MYO1 YOL069w NUF2 YOR058c ASE1 YPL242C IQG1	<b>Chromosome Segregation</b> YBR138c HDR1 YDR150w NUF1* YGR092w DBF2 YHR023w MYO1 YOL069w NUF2 YOR058c ASE1 YPL242C IQG1	<b>Chromosome Segregation</b> YBR138c HDR1 YDR150w NUF1* YGR092w DBF2 YHR023w MYO1 YOL069w NUF2 YOR058c ASE1 YPL242C IQG1	<b>Chromosome Segregation</b> YBR138c HDR1 YDR150w NUF1* YGR092w DBF2 YHR023w MYO1 YOL069w NUF2 YOR058c ASE1 YPL242C IQG1	<b>Chromosome Segregation</b> YBR138c HDR1 YDR150w NUF1* YGR092w DBF2 YHR023w MYO1 YOL069w NUF2 YOR058c ASE1 YPL242C IQG1	<b>Chromosome Segregation</b> YBR138c HDR1 YDR150w NUF1* YGR092w DBF2 YHR023w MYO1 YOL069w NUF2 YOR058c ASE1 YPL242C IQG1	<b>Chromosome Segregation</b> YBR138c HDR1 YDR150w NUF1* YGR092w DBF2 YHR023w MYO1 YOL069w NUF2 YOR058c ASE1 YPL242C IQG1	<b>Chromosome Segregation</b> YBR138c HDR1 YDR150w NUF1* YGR092w DBF2 YHR023w MYO1 YOL069w NUF2 YOR058c ASE1 YPL242C IQG1	<b>Chromosome Segregation</b> YBR138c HDR1 YDR150w NUF1* YGR092w DBF2 YHR023w MYO1 YOL069w NUF2 YOR058c ASE1 YPL242C IQG1	<b>Chromosome Segregation</b> YBR138c HDR1 YDR150w NUF1* YGR092w DBF2 YHR023w MYO1 YOL069w NUF2 YOR058c ASE1 YPL242C IQG1	<b>Chromosome Segregation</b> YBR138c HDR1 YDR150w NUF1* YGR092w DBF2 YHR023w MYO1 YOL069w NUF2 YOR058c ASE1 YPL242C IQG1	<b>Chromosome Segregation</b> YBR138c HDR1 YDR150w NUF1* YGR092w DBF2 YHR023w MYO1 YOL069w NUF2 YOR058c ASE1 YPL242C IQG1	<b>Chromosome Segregation</b> YBR138c HDR1 YDR150w NUF1* YGR092w DBF2 YHR023w MYO1 YOL069w NUF2 YOR058c ASE1 YPL242C IQG1	<b>Chromosome Segregation</b> YBR138c HDR1 YDR150w NUF1* YGR092w DBF2 YHR023w MYO1 YOL069w NUF2 YOR058c ASE1 YPL242C IQG1	<b>Chromosome Segregation</b> YBR138c HDR1 YDR150w NUF1* YGR092w DBF2 YHR023w MYO1 YOL069w NUF2 YOR058c ASE1 YPL242C IQG1	<b>Chromosome Segregation</b> YBR138c HDR1 YDR150w NUF1* YGR092w DBF2 YHR023w MYO1 YOL069w NUF2 YOR058c ASE1 YPL242C IQG1	<b>Chromosome Segregation</b> YBR138c HDR1 YDR150w NUF1* YGR092w DBF2 YHR023w MYO1 YOL069w NUF2 YOR058c ASE1 YPL242C IQG1	<b>Chromosome Segregation</b> YBR138c HDR1 YDR150w NUF1* YGR092w DBF2 YHR023w MYO1 YOL069w NUF2 YOR058c ASE1 YPL242C IQG1	<b>Chromosome Segregation</b> YBR138c HDR1 YDR150w NUF1* YGR092w DBF2 YHR023w MYO1 YOL069w NUF2 YOR058c ASE1 YPL242C IQG1	<b>Chromosome Segregation</b> YBR138c HDR1 YDR150w NUF1* YGR092w DBF2 YHR023w MYO1 YOL069w NUF2 YOR058c ASE1 YPL242C IQG1	<b>Chromosome Segregation</b> YBR138c HDR1 YDR150w NUF1* YGR092w DBF2 YHR023w MYO1 YOL069w NUF2 YOR058c ASE1 YPL242C IQG1	<b>Chromosome Segregation</b> YBR138c HDR1 YDR150w NUF1* YGR092w DBF2 YHR023w MYO1 YOL069w NUF2 YOR058c ASE1 YPL242C IQG1	<b>Chromosome Segregation</b> YBR138c HDR1 YDR150w NUF1* YGR092w DBF2 YHR023w MYO1 YOL069w NUF2 YOR058c ASE1 YPL242C IQG1	<b>Chromosome Segregation</b> YBR138c HDR1 YDR150w NUF1* YGR092w DBF2 YHR023w MYO1 YOL069w NUF2 YOR058c ASE1 YPL242C IQG1	<b>Chromosome Segregation</b> YBR138c HDR1 YDR150w NUF1* YGR092w DBF2 YHR023w MYO1 YOL069w NUF2 YOR058c ASE1 YPL242C IQG1	<b>Chromosome Segregation</b> YBR138c HDR1 YDR150w NUF1* YGR092w DBF2 YHR023w MYO1 YOL069w NUF2 YOR058c ASE1 YPL242C IQG1	<b>Chromosome Segregation</b> YBR138c HDR1 YDR150w NUF1* YGR092w DBF2 YHR023w MYO1 YOL069w NUF2 YOR058c ASE1 YPL242C IQG1	<b>Chromosome Segregation</b> YBR138c HDR1 YDR150w NUF1* YGR092w DBF2 YHR023w MYO1 YOL069w NUF2 YOR058c ASE1 YPL242C IQG1	<b>Chromosome Segregation</b> YBR138c HDR1 YDR150w NUF1* YGR092w DBF2 YHR023w MYO1 YOL069w NUF2 YOR058c ASE1 YPL242C IQG1	<b>Chromosome Segregation</b> YBR138c HDR1 YDR150w NUF1* YGR092w DBF2 YHR023w MYO1 YOL069w NUF2 YOR058c ASE1 YPL242C IQG1	<b>Chromosome Segregation</b> YBR138c HDR1 YDR150w NUF1* YGR092w DBF2 YHR023w MYO1 YOL069w NUF2 YOR058c ASE1 YPL242C IQG1	<b>Chromosome Segregation</b> YBR138c HDR1 YDR150w NUF1* YGR092w DBF2 YHR023w MYO1 YOL069w NUF2 YOR058c ASE1 YPL242C IQG1	<b>Chromosome Segregation</b> YBR138c HDR1 YDR150w NUF1* YGR092w DBF2 YHR023w MYO1 YOL069w NUF2 YOR058c ASE1 YPL242C IQG1	<b>Chromosome Segregation</b> YBR138c HDR1 YDR150w NUF1* YGR092w DBF2 YHR023w MYO1 YOL069w NUF2 YOR058c ASE1 YPL242C IQG1	<b>Chromosome Segregation</b> YBR138c HDR1 YDR150w NUF1* YGR092w DBF2 YHR023w MYO1 YOL069w NUF2 YOR058c ASE1 YPL242C IQG1	<b>Chromosome Segregation</b> YBR138c HDR1 YDR150w NUF1* YGR092w DBF2 YHR023w MYO1 YOL069w NUF2 YOR058c ASE1 YPL242C IQG1	<b>Chromosome Segregation</b> YBR138c HDR1 YDR150w NUF1* YGR092w DBF2 YHR023w MYO1 YOL069w NUF2 YOR058c ASE1 YPL242C IQG1	<b>Chromosome Segregation</b> YBR138c HDR1 YDR150w NUF1* YGR092w DBF2 YHR023w MYO1 YOL069w NUF2 YOR058c ASE1 YPL242C IQG1	<b>Chromosome Segregation</b> YBR138c HDR1 YDR150w NUF1* YGR092w DBF2 YHR023w MYO1 YOL069w NUF2 YOR058c ASE1 YPL242C IQG1	<b>Chromosome Segregation</b> YBR138c HDR1 YDR150w NUF1* YGR092w DBF2 YHR023w MYO1 YOL069w NUF2 YOR058c ASE1 YPL242C IQG1	<b>Chromosome Segregation</b> YBR138c HDR1 YDR150w NUF1* YGR092w DBF2 YHR023w MYO1 YOL069w NUF2 YOR058c ASE1 YPL242C IQG1	<b>Chromosome Segregation</b> YBR138c HDR1 YDR150w NUF1* YGR092w DBF2 YHR023w MYO1 YOL069w NUF2 YOR058c ASE1 YPL242C IQG1	<b>Chromosome Segregation</b> YBR138c HDR1 YDR150w NUF1* YGR092w DBF2 YHR023w MYO1 YOL069w NUF2 YOR058c ASE1 YPL242C IQG1	<b>Chromosome Segregation</b> YBR138c HDR1 YDR150w NUF1* YGR092w DBF2 YHR023w MYO1 YOL069w NUF2 YOR058c ASE1 YPL242C IQG1	<b>Chromosome Segregation</b> YBR138c HDR1 YDR150w NUF1* YGR092w DBF2 YHR023w MYO1 YOL069w NUF2 YOR058c ASE1 YPL242C IQG1	<b>Chromosome Segregation</b> YBR138c HDR1 YDR150w NUF1* YGR092w DBF2 YHR023w MYO1 YOL069w NUF2 YOR058c ASE1 YPL242C IQG1	<b>Chromosome Segregation</b> YBR138c HDR1 YDR150w NUF1* YGR092w DBF2 YHR023w MYO1 YOL069w NUF2 YOR058c ASE1 YPL242C IQG1	<b>Chromosome Segregation</b> YBR138c HDR1 YDR150w NUF1* YGR092w DBF2 YHR023w MYO1 YOL069w NUF2 YOR058c ASE1 YPL242C IQG1	<b>Chromosome Segregation</b> YBR138c HDR1 YDR150w NUF1* YGR092w DBF2 YHR023w MYO1 YOL069w NUF2 YOR058c ASE1 YPL242C IQG1	<b>Chromosome Segregation</b> YBR138c HDR1 YDR150w NUF1* YGR092w DBF2 YHR023w MYO1 YOL069w NUF2 YOR058c ASE1 YPL242C IQG1	<b>Chromosome Segregation</b> YBR138c HDR1 YDR150w NUF1* YGR092w DBF2 YHR023w MYO1 YOL069w NUF2 YOR058c ASE1 YPL242C IQG1	<b>Chromosome Segregation</b> YBR138c HDR1 YDR150w NUF1* YGR092w DBF2 YHR023w MYO1 YOL069w NUF2 YOR058c ASE1 YPL242C IQG1	<b>Chromosome Segregation&lt;/</b>
-----------------------------------	-----------------------------------	---	---	---	--	--	--	--	--	--	--	--	--	--	--	--	--	--	--	--	--	--	--	--	--	--	--	--	--	--	--	--	--	--	--	--	--	--	--	--	--	--	--	--	--	--	--	--	--	--	--	--	--	--	--	--	--	--	--	--	--	--	--	--	--	--	--	--	--	--	--	--	--	--	--	--	--	------------------------------------

Functionally characterized genes whose transcripts display periodic fluctuation are listed according to their biological function. The MIPS data base was used to determine which genes have been characterized. Under each phase heading, the number of characterized genes that peak only in that category is listed as a proportion of the total genes in that category. The category of Chromosome Segregation includes the process of nuclear division. Genes that peak in more than one cell cycle phase are listed under both phases and marked with an asterisk (\*).





Figure 3. Genome-Wide Map of Physical Locations of Genes that Display Cell Cycle-Dependent mRNA Fluctuation  
See text for further details.

sequence, G2 and M regulatory elements may be relatively rare, but highly specific in determining mRNA fluctuation. Alternatively, regulatory sequences that affect transcription during these periods may be relatively degenerate. Another explanation for transcript fluctuation during the cell cycle is that some transcripts may display differential stability. For example, it is known that mammalian histone mRNA is destabilized at the end of S phase (Ross, 1995). Both methods described here for identifying candidate regulatory elements will become increasingly relevant as additional genome-wide transcription data is generated. Further investigation will be needed to assess the role of candidate regulatory sequences suggested by these experiments.

The chromosomal position of genes can strongly influence their transcription, as observed in the silencing of genes in telomeric regions (Shore, 1997). Little evidence was observed for a direct correlation between telomeric or centromeric gene location and mRNA fluctuation during the cell cycle. However, more than 25% of all genes displaying periodic transcript levels were positioned directly adjacent to another gene induced in the same cell cycle phase (Figure 3). The proportion of cell cycle-regulated genes that would occupy adjacent positions by random chance is less than 5%. Because many eukaryotic transcription factor-binding sites are either nearly palindromic or are active on both strands, it is possible that these gene pairs are regulated by the same upstream sequence. Consistent with this hypothesis, 51% of these gene pairs are transcribed divergently on opposite strands, many with fewer than 1500 bp bases separating their 5' ends. 38% of adjacent genes were transcribed in the same orientation, while only 11% were transcribed convergently. Fewer than 25% of the adjacent gene pairs that were divergently transcribed displayed different patterns of mRNA fluctuation. This suggests that in genomes with limited intergenic sequence,

sharing of upstream regulatory elements may be an important determinant of global mRNA regulation. It is also possible that the clustering of cell cycle-regulated genes results from local positional effects that are not sequence dependent. For example, the restructuring of chromosomes during cell cycle events such as DNA replication may affect the transcription of genes at specific chromosomal positions.

The biochemical functions of genes displaying periodic mRNA fluctuation were examined. Consistent with previous studies, cell cycle-dependent changes in transcript level were observed for the *CLN* and *CLB* cyclin families, transcription factors, and gene products involved in DNA replication and packaging (Figures 4A and 4B) (Wittenberg et al., 1990; Koch and Nasmyth, 1994). The resolution of these experiments was sufficient to distinguish induction of the *MCM* genes and *CDC6*, which are involved in formation of the prereplication complex (pre-RC) during early G1, from the DNA polymerase subunits, DNA replication factors, and the S phase cyclin *CLB5*, which are induced in late G1 (Figure 4C). The kinetic separation is biologically significant because it reflects the need for the prereplication complex to be assembled prior to production of the S phase cyclins (Stillman, 1996). Activation of S phase cyclins permits exactly one round of DNA replication by simultaneously driving origin firing and inhibiting the reassembly of the prereplication complex. It is likely that additional clues to functional genetic relationships reside in these transcriptional data.

As expected, genes encoding constituents of a protein complex were generally coregulated. The DNA replication factors *RFA1*, *RFA2*, and *RFA3* displayed nearly identical patterns of mRNA fluctuation. However, mRNA levels of components of the spindle pole body were induced in different cell cycle phases, perhaps reflecting distinct temporal roles for these genes.

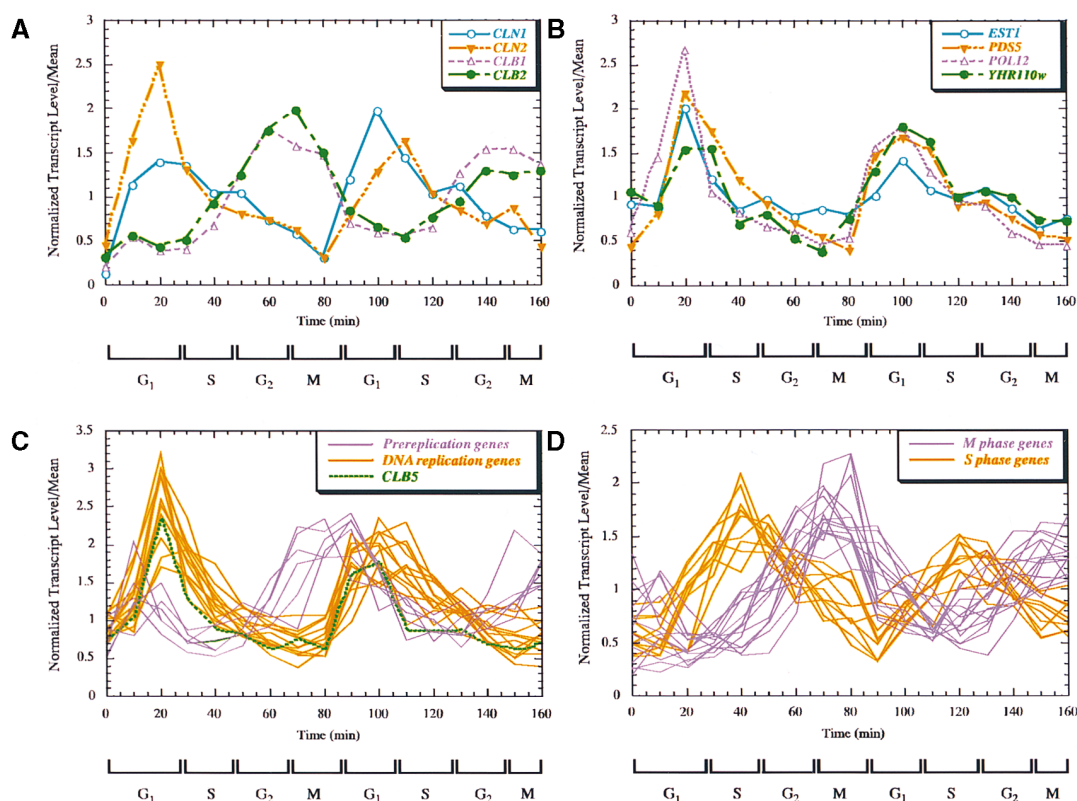


Figure 4. Fluctuation of Transcript Levels during Mitosis

Graphs of normalized transcript level divided by mean value against time for: (a) transcripts for the *CLN1*, *CLN2*, *CLB1*, and *CLB2* cyclin genes; (b) transcripts for *EST1*, *PDS5*, *POL12*, and *YHR110w*; (c) transcripts for *CLB5*, the prereplication genes *CDC6*, *CDC46*, *CDC47*, *CDC54*, *MCM2*, and *MCM3*, and the DNA replication genes *CDC17*, *CDC21*, *DPB2*, *DPB3*, *POL2*, *POL12*, *POL30*, *PRF1*, *RFA1*, *RFA2*, and *RNR1*; (d) the S phase transcripts *CIN8*, *KIP1*, *SPC98*, *STU2*, *SWI1*, *YBR156c*, *YDR219c*, *YER018c*, *YJL118w*, and *YNL176c*, and the M phase transcripts *ACE2*, *CLB1*, *CLB2*, *CDC5*, *DBF2*, *HDR1*, *HST3*, *MCM6*, *MYO3*, *PRY1*, *SKN1*, *TSM1*, and *WTM3*.

Periodic mRNA fluctuation was also observed in functional classifications of genes not previously associated with the cell cycle. For example, transcripts for the *FAA1*, *FAA3*, and *ELO1* enzymes, which participate in fatty acid biosynthesis, peaked during G<sub>1</sub>. Many of the nuclear-encoded mitochondrial enzymes required for glycolysis and oxidative phosphorylation were induced in early G<sub>1</sub> with very similar patterns of mRNA fluctuation. None of the transcripts for these mitochondrial genes peaked outside of G<sub>1</sub>.

Because proteolysis is known to be a critical factor in regulating progression of the cell cycle, transcripts of both proteolytic effectors and substrates were examined for periodic changes in transcript levels. No periodic fluctuation was observed for any transcripts encoding constituents of the anaphase-promoting complex (APC), the *CDC34* complex, or ubiquitin-dependent degradation pathway, which are involved in the proteolytic degradation of key cell cycle regulators at the onset of anaphase and the onset of DNA replication (King et al., 1996; Deshaies, 1997; Irniger and Nasmyth, 1997; Osaka et al., 1997; Page and Hieter, 1997; Verma et al., 1997; Yew and Kirschner, 1997). As previously reported, the transcripts of all known proteolytic substrates displayed cell cycle-dependent periodicity. However, the resolution of these experiments allowed direct comparison

between patterns of mRNA fluctuation. For example, the transcripts of the APC substrates *ASE1* and *CLB2* displayed identical kinetics of decay during G<sub>1</sub>, while the transcript of the APC substrate *PDS1* showed a distinct pattern of decay during S phase. Interestingly, *ASE1* and *CLB2* are degraded by the same APC pathway, while the degradation of *PDS1* seems to involve distinct regulatory components (Visintin et al., 1997). These results suggest that attenuation of gene activity on the mRNA and protein levels may be coordinately regulated.

It has been proposed that mRNA and protein expression patterns may provide clues to the function of previously uncharacterized genes (Lander, 1996). To assess the likelihood that uncharacterized genes found in our screen play a cell cycle period-specific role, the correlation between mRNA fluctuation and gene function was examined. More than 60% of the characterized genes that displayed cell cycle-dependent mRNA fluctuation have been previously implicated in cell cycle period-specific biological activities. Therefore, mRNA regulation is a strong indicator of biological function in the cell cycle, and it is likely that many of the uncharacterized genes in this screen have functions related to the cell cycle. However, periodicity of mRNA abundance was observed in fewer than 25% of all known *CDC* genes

Table 2. Established and Candidate Upstream Regulatory Elements

Number of Genes Examined		Early G <sub>1</sub> 63	Late G <sub>1</sub> 134	S 74	G <sub>2</sub> 56	M 56	Genome 5519
Promoter Element	5'-3' Sequence						
MCB	ACGCTNA	6 (9.2)	53 (39)	11 (14)	0 (0)	0 (0)	111 (2.0)
SCB	CACGAA	15 (23)	26 (19)	20 (26)	8 (14)	5 (8.9)	931 (15)
ECB	TTWCCCNNNAGGAA	8 (12)	1 (0.7)	0 (0)	0 (0)	1 (1.8)	5 (0.1)
in text	AAAANGTAAACAA	0 (0)	1 (0.8)	1 (1.4)	5 (8.9)	4 (7.1)	8 (0.01)
in text (MCM1-based)	TWTNWCCYAAANNNGNNA	0 (0)	0 (0)	0 (0)	6 (11)	0 (0)	0 (0)
Hexamers	CCCCGC	13 (21)	3 (2.2)	2 (2.7)	1 (1.8)	1 (1.8)	320 (5.8)
	ACGCGG	8 (13)	3 (2.2)	6 (8.1)	0 (0)	0 (0)	283 (5.1)
	ACGCGT	8 (13)	64 (48)	16 (22)	0 (0)	1 (1.8)	222 (4.0)
	AACGCG	11 (17)	68 (51)	22 (30)	2 (3.6)	1 (1.8)	543 (9.8)
	CGTCTC	0 (0)	19 (14)	11 (15)	2 (3.6)	0 (0)	533 (9.7)
	GCGAAA	13 (21)	57 (43)	33 (45)	21 (38)	8 (14)	1265 (23)
	GAGTCA	2 (3.2)	4 (3.0)	7 (9.5)	13 (23)	5 (9.0)	740 (13)
	CGCGCG	1 (1.6)	4 (3.0)	3 (4.1)	9 (16)	1 (1.8)	150 (2.7)
	AAACCC	10 (16)	14 (10)	6 (8.1)	13 (23)	24 (43)	1031 (19)
	ACTCTC	7 (11)	16 (12)	8 (11)	4 (7.1)	17 (30)	893 (16)

Regulatory sequences (5' to 3') and their frequency of occurrence in the 500 bp upstream of genes that display cell cycle-dependent mRNA fluctuation are listed. Genes with more than one transcriptional peak were not considered for these calculations. The last 10 sequences are the hexamers that show the greatest bias toward the promoters of genes in each cell cycle category. Both strands were searched for regulatory sequences. Calculations for the MCM1-bases site involve upstream regions greater than 500 bp. Frequency of sites is also shown for 5519 non-cell cycle-regulated genes in the yeast genome. Percentage of genes in each category containing the regulatory sequence is listed in parentheses.

and genes known to be involved in budding, DNA replication, or other cell cycle period-specific biological roles. Many of the genes that do not display periodic transcript levels are known to be modulated at the post-translational level. It has also been established that the constitutive transcription of some genes with periodic transcript levels do not result in an obvious phenotype (Koch and Nasmyth, 1994). These results strongly emphasize the need for multiple approaches in elucidating the function of uncharacterized genes. It is likely that additional aspects of coordinate mRNA regulation await discovery from this data set. We encourage the reader to explore the data base, which can be viewed at the internet address given above.

#### Experimental Procedures

All *S. cerevisiae* strains used in this study were derived from the W101 genetic background. Strain K3445 (YNN553) contains the *cdc28-13* allele and strain K2944 (YNN554) contains the *cdc15-2* allele (kindly provided by K. Nasmyth). Strain K3445 was grown overnight in YPAD (yeast extract/adenine/peptone/glucose, Difco Laboratories, Detroit, MI) at 25°C to a density of  $8.0 \times 10^6$  cells/ml and divided into 50 ml aliquots. Cells were diluted in the evening so that on the following morning, their density would be appropriate for heat shock and arrest. On the following morning, all samples were transferred to a 37°C shaking waterbath for 165 min. The cell cycle was reinitiated by moving the flasks to a 25°C shaking waterbath. Every 10 min, one 50 ml sample was centrifuged for 2 min at 25°C, frozen in liquid nitrogen, and stored at -80°C until use. An identical time course was carried out for 50 ml cultures of strain K2944, and cells were frozen at -80°C until further use.

Frozen cell pellets were thawed by vortexing with 5 ml of neutral phenol (USB Laboratories, Cleveland, OH) and 5 ml of 75 mM NH<sub>4</sub>OAc, 10 mM EDTA. Cells were broken by vortexing vigorously for 5 min with 5 g of 0.5 mm glass beads in 30 ml polypropylene tubes (Nalgene, Rochester, NY). Extraction with phenol was followed by an extraction with an equal volume of phenol:chloroform. Following ethanol precipitation of nucleic acid, poly(A)<sup>+</sup> RNA was purified from total RNA with an Oligotex dT-column selection step (Qiagen,

Chatsworth, CA). Purified poly(A)<sup>+</sup> RNA appeared undegraded on an agarose gel. Ribosomal bands were substantially reduced, and the final poly(A)<sup>+</sup> RNA yield was approximately 1.2% of total RNA. Reverse transcription reactions were performed using 20 µg of poly(A)<sup>+</sup> RNA, 2 nmol of oligo dT21 primer, 10 mM DTT, 1st Strand Buffer (GIBCO Life Technologies, Gaithersburg, MD), 400 µM of each dNTP (New England Biolabs), and 4000 U of Superscript II Reverse Transcriptase (GIBCO). RNA and primer were annealed for 10 min at 65°C, and the reaction was incubated at 42°C for 60 min.

For second-strand synthesis, the following components were added to reverse transcription reactions: 120 µl of 5× 2nd Strand Buffer (GIBCO), 110 nmol of each dNTP, 12 U of RNase H (GIBCO), 160 U of *E. coli* DNA polymerase I (GIBCO), and 40 U of *E. coli* DNA ligase (New England Biolabs, Beverly, MA). The 600 µl reaction volume was incubated at 16°C for 180 min. 30 U of T4 DNA polymerase (GIBCO) was added to each reaction for 5 min at 16°C. Reactions were extracted with an equal volume of phenol:chloroform. Phase-Lock Gel (5 Prime-3Prime, Inc., Boulder, CO) was used for all organic extractions to increase DNA recovery and decrease the potential for contamination with material from the organic interface. Double-stranded cDNA was ethanol precipitated and resuspended in 30 µl of distilled water. cDNA was fragmented to an average length of 50 bp with addition of 3.5 µl of One-Phor-All buffer (Pharmacia Biotech, Piscataway, NJ), 2.2 µl of 25 mM CoCl<sub>2</sub> (Boehringer Mannheim, Indianapolis, IN), and 0.15 U of amplification-grade DNase I (GIBCO). Reactions were incubated at 37°C for 5 min and terminated by incubation in a boiling water bath for 15 min. Following boiling, reactions were immediately chilled on ice. DNA fragments were 3' end-labeled by a 2 hr incubation at 37°C after addition of 1.25 nmol of biotin-N<sub>6</sub>-ddATP (DuPont NEN, Boston, MA) and 25 U of terminal transferase (Boehringer Mannheim).

A set of four oligonucleotide arrays containing a total of more than 260,000 oligonucleotides complementary to 6,218 yeast genes were used for quantitation of labeled cDNA (Affymetrix). End-labeled and fragmented cDNA was diluted to 200 µl using a hybridization solution containing 1.0 M NaCl, 10 mM Tris-HCl (pH 7.6), and 0.005% Triton X-100 (referred to as ST-T). In addition, the solutions contained 0.1 mg/ml unlabeled, sonicated herring sperm DNA (Promega). cDNA samples were heated for 99°C for 2 min and cooled to room temperature before being placed in the hybridization cartridge. Hybridizations were carried out at 42°C for 14-16 hr with mixing on a rotisserie at 60 rpm. Following hybridization, the solutions were removed, the arrays were rinsed with 6× SSPE-T (0.9 M NaCl, 60

mM NaH<sub>2</sub>PO<sub>4</sub>, 6 mM EDTA, 0.005% Triton X-100 adjusted to pH 7.6), rinsed with 0.5× SSPE-T (75 mM NaCl, 5 mM NaH<sub>2</sub>PO<sub>4</sub>, 0.5 mM EDTA, 0.005% Triton X-100 adjusted to pH 7.6), and incubated with 0.5× SSPE-T at 42°C for 15 min. Following washing, the hybridized biotinylated DNA was fluorescently labeled by incubating with 2 µg/ml streptavidin-phycoerythrin (Molecular Probes, Eugene, OR) and 1 mg/ml acetylated BSA (Sigma, St. Louis, MO) in 6× SSPE-T at 42°C for 10 min. Unbound streptavidin-phycoerythrin was removed by rinsing at room temperature prior to scanning. The arrays were read at a resolution of 7.5 µm using a specially designed confocal scanner (Affymetrix, Santa Clara, CA) as described previously (Wodicka et al., 1997).

The cell cycle phase of a particular sample was determined using the size of the bud, the position of the nucleus inside the cell, and the induction pattern of a number of well-characterized transcripts. Bud size was determined as unbudded, small-budded, or large-budded. Bud size as a percentage of mother cell size was calculated after measuring buds and mother cells from photographs using a ruler. The criterion for a small bud was that it should occupy less than 70% of the surface area of the mother cell. The criterion for a large bud was that it should occupy more than 70% of the mother cell. The error in measurement was not more than 10% of total bud size. After DAPI staining, a cell was determined as mitotic if the nucleus was at least partly straddling the bud neck. A cell was determined as postmitotic if the nucleus was separated between the mother and daughter cells. Postmitotic cells were considered to be in G1. A cell was considered to be premitotic if the nucleus had not yet migrated to the bud neck.

Because cells were analyzed over two cell cycles, postmitotic cells from the first division needed to be reset at some point to a premitotic cell of the second division. The most appropriate time to make this reset was at 110 min. The beginning of S phase was delineated using the appearance of buds, and the end of S phase was determined by the attainment of the large budded state and the appearance of certain transcripts (see below) for the end of S phase.

As landmarks in our time course, 25 transcripts were previously characterized with respect to a specific cell cycle phase. These transcripts were used to confirm delineations of cell cycle phases based on morphological markers. For landmarks in late G1, the following genes were used: *CDC9* (DNA ligase), *CLN1*, *CLN2*, *CLB5*, *CLB6*, *RNR1* (ribonucleotide reductase), and *CDC21* (thymidylate synthase). For landmarks in early G1, the following genes were used: *SIC1* (*CDC28* inhibitor), and the prereplication complex genes *CDC6*, *CDC46*, and *CDC47*. For S phase the following genes were used: the histone genes *HTA*, *HTB*, *HHT*, *HHF*, *SPC97*, and *SPC98*. For landmarks in G2 phase the following genes were used: *DBF20* and *BUD3*. For landmarks in M phase the following genes were used: *ACE2*, *SWI5*, *CLB1*, *CLB2*, *CLN3*, and *DBF2*.

## Acknowledgments

We thank the labs of Frederick Cross and Kim Nasmyth for providing reagents. Helpful comments were provided by Tim Stearns, Daria Siekhaus, and Eunice Yoon. This work was supported by a National Institutes of Health Institutional Training Grant in Genome Science.

Received March 25, 1998; revised June 4, 1998.

## References

Althoefer, H., Schleiffer, A., Wassmann, K., Nordheim, A., and Ammerer, G. (1995). Mcm1 is required to coordinate G2-specific transcription in *Saccharomyces cerevisiae*. *Mol. Cell. Biol.* **15**, 5917–5928.

Andrews, B.J., and Herskowitz, I. (1989). The yeast *SWI4* protein contains a motif present in developmental regulators and is part of a complex involved in cell-cycle-dependent transcription. *Nature* **342**, 830–833.

Brazas, R.M., and Stillman, D.J. (1993). The *Swi5* zinc-finger and *Grf10* homeodomain proteins bind DNA cooperatively at the yeast *HO* promoter. *Proc. Natl. Acad. Sci. USA* **90**, 11237–11241.

Breedon, L., and Nasmyth, K. (1987). Cell cycle control of the yeast *HO* gene: *Cis*- and *Trans*-acting regulators. *Cell* **48**, 389–397.

DeRisi, J.L., Iyer, V.R., and Brown, P.O. (1997). Exploring the metabolic and genetic control of gene expression on a genomic scale. *Science* **278**, 680–686.

Deshaies, R.J. (1997). Phosphorylation and proteolysis: partners in the regulation of cell division in budding yeast. *Curr. Opin. Genet. Dev.* **7**, 7–16.

Dong, X., Zavitz, K.H., Thomas, B.J., Lin, M., Campbell, S., and Zipursky, S.L. (1997). Control of G1 in the developing *Drosophila* eye: *rca1* regulates Cyclin A. *Genes Dev.* **11**, 94–105.

Gönczy, P., Thomas, B.J., and DiNardo, S. (1994). *roughex* is a dose-dependent regulator of the second meiotic division during *Drosophila* spermatogenesis. *Cell* **77**, 1015–1025.

Hall, M., and Peters, G. (1996). Genetic alterations of cyclins, cyclin-dependent kinases, and Cdk inhibitors in human cancer. *Adv. Cancer Res.* **68**, 67–108.

Hartwell, L.H., and Kastan, M.B. (1994). Cell cycle control and cancer. *Science* **266**, 1821–1828.

Hunter, T., and Pines, J. (1994). Cyclins and cancer. II: cyclin D and CDK inhibitors come of age. *Cell* **79**, 573–582.

Irniger, S., and Nasmyth, K. (1997). The anaphase-promoting complex is required in G1 arrested yeast cells to inhibit B-type cyclin accumulation and to prevent uncontrolled entry into S-phase. *J. Cell Sci.* **110**, 1523–1531.

Jang, J.K., Messina, L., Erdman, M.B., Arbel, T., and Hawley, R.S. (1995). Induction of metaphase arrest in *Drosophila* oocytes by chiasma-based kinetochore tension. *Science* **268**, 1917–1919.

King, R.W., Deshaies, R.J., Peters, J.M., and Kirschner, M.W. (1996). How proteolysis drives the cell cycle. *Science* **274**, 1652–1659.

Koch, C., and Nasmyth, K. (1994). Cell cycle regulated transcription in yeast. *Curr. Opin. Cell Biol.* **6**, 451–459.

Lander, E.S. (1996). The new genomics: global views of biology. *Science* **274**, 536–539.

Lashkari, D.A., McCusker, J.H., and Davis, R.W. (1997). Whole genome analysis: experimental access to all genome sequenced segments through larger-scale efficient oligonucleotide synthesis and PCR. *Proc. Natl. Acad. Sci. USA* **94**, 8945–8947.

McBride, H.J., Brazas, R.M., Yu, Y., Nasmyth, K., and Stillman, D.J. (1997). Long-range interactions at the *HO* promoter. *Mol. Cell. Biol.* **17**, 2669–2678.

McInerney, C.J., Partridge, J.F., Mikesell, G.E., Creemer, D.P., and Breedon, L.L. (1997). A novel Mcm1-dependent element in the *SWI4*, *CLN3*, *CDC6*, and *CDC47* promoters activates M/G1-specific transcription. *Genes Dev.* **11**, 1277–1288.

Nasmyth, K. (1985). A repetitive DNA sequence that confers cell-cycle START (*CDC28*)-dependent transcription of the *HO* gene in yeast. *Cell* **42**, 225–235.

Oehlen, L.J., and Cross, F.R. (1994). G1 cyclins *CLN1* and *CLN2* repress the mating factor response pathway at Start in the yeast cell cycle. *Genes Dev.* **8**, 1058–1070.

Oehlen, L.J., McKinney, J.D., and Cross, F.R. (1996). Ste12 and Mcm1 regulate cell cycle-dependent transcription of *FAR1*. *Mol. Cell. Biol.* **16**, 2830–2837.

Ogas, J., Andrews, B.J., and Herskowitz, I. (1991). Transcriptional activation of *CLN1*, *CLN2*, and a putative new G1 cyclin (*HCS26*) by *SWI4*, a positive regulator of G1-specific transcription. *Cell* **66**, 1015–1026.

Osaka, F., Seino, H., Seno, T., and Yamao, F. (1997). A ubiquitin-conjugating enzyme in fission yeast that is essential for the onset of anaphase in mitosis. *Mol. Cell. Biol.* **17**, 3388–3397.

Page, A.M., and Hieter, P. (1997). The anaphase promoting complex. *Cancer Surv.* **29**, 133–150.

Painter, R.B., and Young, B.R. (1980). Radiosensitivity in ataxia-telangiectasia: a new explanation. *Proc. Natl. Acad. Sci. USA* **77**, 7315–7317.

Ross, J. (1995). mRNA stability in mammalian cells. *Microbiol. Rev.* **59**, 423–450.

Sanders, S.L., and Herskowitz, I. (1996). The *BUD4* protein of yeast,



- required for axial budding, is localized to the mother/BUD neck in a cell cycle-dependent manner. *J. Cell Biol.* 134, 413–427.
- Scully, R., Chen, J., Ochs, R.L., Keegan, K., Hoekstra, M., Feunteun, J., and Livingston, D.M. (1997). Dynamic changes of BRCA1 subnuclear location and phosphorylation state are initiated by DNA damage. *Cell* 90, 425–435.
- Sherr, C.J., and Roberts, J.M. (1995). Inhibitors of mammalian G1 cyclin-dependent kinases. *Genes Dev.* 9, 1149–1163.
- Shore, D. (1997). Telomere length regulation: getting the measure of chromosome ends. *Biol. Chem.* 378, 591–597.
- Stillman, B. (1996). Cell cycle control of DNA replication. *Science* 274, 1659–1664.
- Thomas, B.J., Gunning, D.A., Cho, J., and Zipursky, L. (1994). Cell cycle progression in the developing *Drosophila* eye: *roughex* encodes a novel protein required for the establishment of G1. *Cell* 77, 1003–1014.
- Thomas, B.J., Zavitz, K.H., Dong, X., Lane, M.E., Weigmann, K., Finley, R.J., Brent, R., Lehner, C.F., and Zipursky, S.L. (1997). *roughex* down-regulates G2 cyclins in G1. *Genes Dev.* 11, 1289–1298.
- Verlhac, M.H., Kubiak, J.Z., Weber, M., Geraud, G., Colledge, W.H., Evans, M.J., and Maro, B. (1996). Mos is required for MAP kinase activation and is involved in microtubule organization during meiotic maturation in the mouse. *Development* 122, 815–822.
- Verma, R., Annan, R.S., Huddleston, M.J., Carr, S.A., Reynard, G., and Deshaies, R.J. (1997). Phosphorylation of Sic1p by G1 Cdk required for its degradation and entry into S phase. *Science* 278, 455–460.
- Visintin, R., Prinz, S., and Amon, A. (1997). *CDC20* and *CDH1*: a family of substrate-specific activators of APC-dependent proteolysis. *Science* 278, 460–463.
- Wang, T.C., Cardiff, R.D., Zukerberg, L., Lees, E., Arnold, A., and Schmidt, E.V. (1994). Mammary hyperplasia and carcinoma in MMTV-cyclin D1 transgenic mice. *Nature* 369, 669–671.
- Weinert, T. (1997). A DNA damage checkpoint meets the cell cycle engine [comment]. *Science* 277, 1450–1451.
- Weinert, T.A., and Hartwell, L.H. (1988). The *RAD9* gene controls the cell cycle response to DNA damage in *Saccharomyces cerevisiae*. *Science* 241, 317–322.
- Wittenberg, C., Sugimoto, K., and Reed, S.I. (1990). G1-specific cyclins of *S. cerevisiae*: cell cycle periodicity, regulation by mating pheromone, and association with the p34<sup>CDC28</sup> protein kinase. *Cell* 62, 225–237.
- Wodicka, L., Dong, H., Mittmann, M., Ho, M.-H., and Lockhart, D.J. (1997). Genome-wide expression monitoring in *Saccharomyces cerevisiae*. *Nat. Biotechnol.* 15, 1359–1367.
- Wölfel, T., Hauer, M., Schneider, J., Serrano, M., Wölfel, C., Klehmann-Hieb, E., De Plaen, E., Hankeln, T., Meyer zum Buschenfelde, K.-H., and Beach, D. (1995). A p16<sup>INK4a</sup>-insensitive CDK4 mutant targeted by cytolytic T lymphocytes in a human melanoma. *Science* 269, 1281–1284.
- Yew, P.R., and Kirschner, M.W. (1997). Proteolysis and DNA replication: the *CDC34* requirement in the *Xenopus* egg cell cycle. *Science* 277, 1672–1676.
- Zanolari, B., and Riezman, H. (1991). Quantitation of alpha-factor internalization and response during the *Saccharomyces cerevisiae* cell cycle. *Mol. Cell. Biol.* 11, 5251–5258.